

J/ψ production in Ru+Ru and Zr+Zr collisions at $\sqrt{s_{NN}} = 200$ GeV with the STAR experiment

Yan Wang (for the STAR Collaboration)^{a,*}

^aState Key Laboratory of Particle Detection and Electronics, University of Science and Technology of China, Hefei 230026, China,

^bDepartment of Modern Physics, University of Science and Technology of China, Hefei 230026, China,
E-mail: wy157543@mail.ustc.edu.cn

In this contribution, we present the measurements of the inclusive J/ψ yield and elliptic flow (v_2) at midrapidity ($|y| < 1.0$) in Ru+Ru and Zr+Zr collisions at $\sqrt{s_{NN}} = 200$ GeV by the STAR experiment. The centrality and transverse momentum (p_T) dependences of the nuclear modification factor (R_{AA}) are measured with much better precision compared to the previous measurements in Au+Au collisions at the same collision energy. The p_T dependence of inclusive J/ψ elliptic flow (v_2) in the same collision systems at $|y| < 1.0$ are also presented. Two methods, the Scalar-Product method and the event-plane method are used individually to extract the J/ψ v_2 in Zr+Zr and Ru+Ru collisions. The two methods' results are consistent in the overlap p_T range. The measurements of the inclusive J/ψ yield and v_2 are compared to the same results in Au+Au collisions at $\sqrt{s_{NN}} = 200$ GeV, and then physics implications are discussed.

HardProbes2023
26-31 March 2023
Aschaffenburg, Germany

*Speaker

1. Introduction

Lattice QCD, the discrete formulation of quantum chromodynamics, predicts a new state of matter created in ultra-relativistic heavy-ion collisions, where quarks and gluons are no longer confined within hadrons, called the quark-gluon plasma (QGP). The heavy quarks (charm and beauty), which are produced via initial hard partonic scatterings and then experience the full evolution of the QGP, are ideal probes to study the properties of the QGP [1]. Quarkonia are bound states of heavy quarks and their anti-quarks, for example the J/ψ meson ($c\bar{c}$). It has been predicted that the J/ψ production should be suppressed due to the presence of the hot medium and the color-screening effect [2, 3]. The degree of suppression of the quarkonia depends on its binding energy and the properties of the QGP. On the other hand, uncorrelated or correlated charm quarks and anticharm quarks could bind into new J/ψ mesons in the deconfined medium, called the regeneration effect. The dissociation and regeneration effects are expected to depend on the size of collision systems. In 2018, the STAR experiment collected a large statistics sample of isobaric collisions ($^{96}_{44}\text{Ru}+^{96}_{44}\text{Ru}$ and $^{96}_{40}\text{Zr}+^{96}_{40}\text{Zr}$) at $\sqrt{s_{NN}} = 200$ GeV. The system size of the Ru+Ru and Zr+Zr collisions is larger than Cu+Cu but smaller than Au+Au collisions, so it is a unique opportunity to study the collision system dependence of the inclusive J/ψ production.

Besides dissociation and regeneration effects, feed-down from the excited states and cold nuclear matter effects also contribute to the final J/ψ yield. Studying the properties of the QGP via the J/ψ production requires a good understanding of all the hot and cold nuclear matter effects. A precise measurement of J/ψ yield in a wide kinematic range is crucial to have a better understanding of different effects.

Another important observable for studying the properties of the QGP is the azimuthal dependence of J/ψ production. J/ψ mesons produced from regeneration will inherit the flow of charm quarks, while the J/ψ mesons from initial hard partonic scatterings are predicted to have very limited flow. A significant elliptic flow of J/ψ mesons has been observed at LHC energy [4, 5], but in Au+Au collisions at the top RHIC energy, the elliptic flow of J/ψ mesons is consistent with zero within the large uncertainties [6].

2. Analysis and Results

The data used in this analysis are 4 billion events from isobaric collisions at $\sqrt{s_{NN}} = 200$ GeV, collected in 2018 by the STAR experiment. J/ψ candidates are reconstructed in the dielectron decay channel. After implementing event-level and track quality cuts, we identified the electron candidate using TPC (Time Projection Chamber), TOF (Time of Flight), and BEMC (Barrel Electromagnetic Calorimeter) detectors. The Mixed-Event Technique was utilized to address the combinatorial background [7]. In the v_2 analysis, the TPC second-order event plane is used to estimate the reaction plane for the BEMC-triggered events (triggered on a high- p_T electron). Then v_2 is calculated using the definition from [8]. For MB events, v_2 is extracted using the Scalar-Product method [9]. The Q-vector of J/ψ is defined as $Q_{2,J/\psi} = e^{in\varphi}$, where φ represents the azimuthal angle. $Q_{2,EPD}$ represents the event flow vector in the EPD (Event Plane Detector). v_2^{SP} is obtained using Eq. 1,

$$v_2^{SP} = \frac{\langle Q_{2,J/\psi} Q_{2,EPD}^* \rangle}{\sqrt{\frac{\langle Q_{2,EPD} Q_{2,TPCW}^* \rangle \langle Q_{2,EPD} Q_{2,TPCE}^* \rangle}{\langle Q_{2,TPCW} Q_{2,TPCE}^* \rangle}}} \quad (1)$$

where $Q_{2,TPCW}$ and $Q_{2,TPCE}$ are the 2nd harmonic event flow vectors measured in the TPC. The *J/ψ* candidate is constructed using TPC, while $Q_{2,EPD}$ is constructed using the EPD. The large pseudorapidity (η) gap between the TPC and EPD significantly reduces non-flow contributions to our final v_2 results.

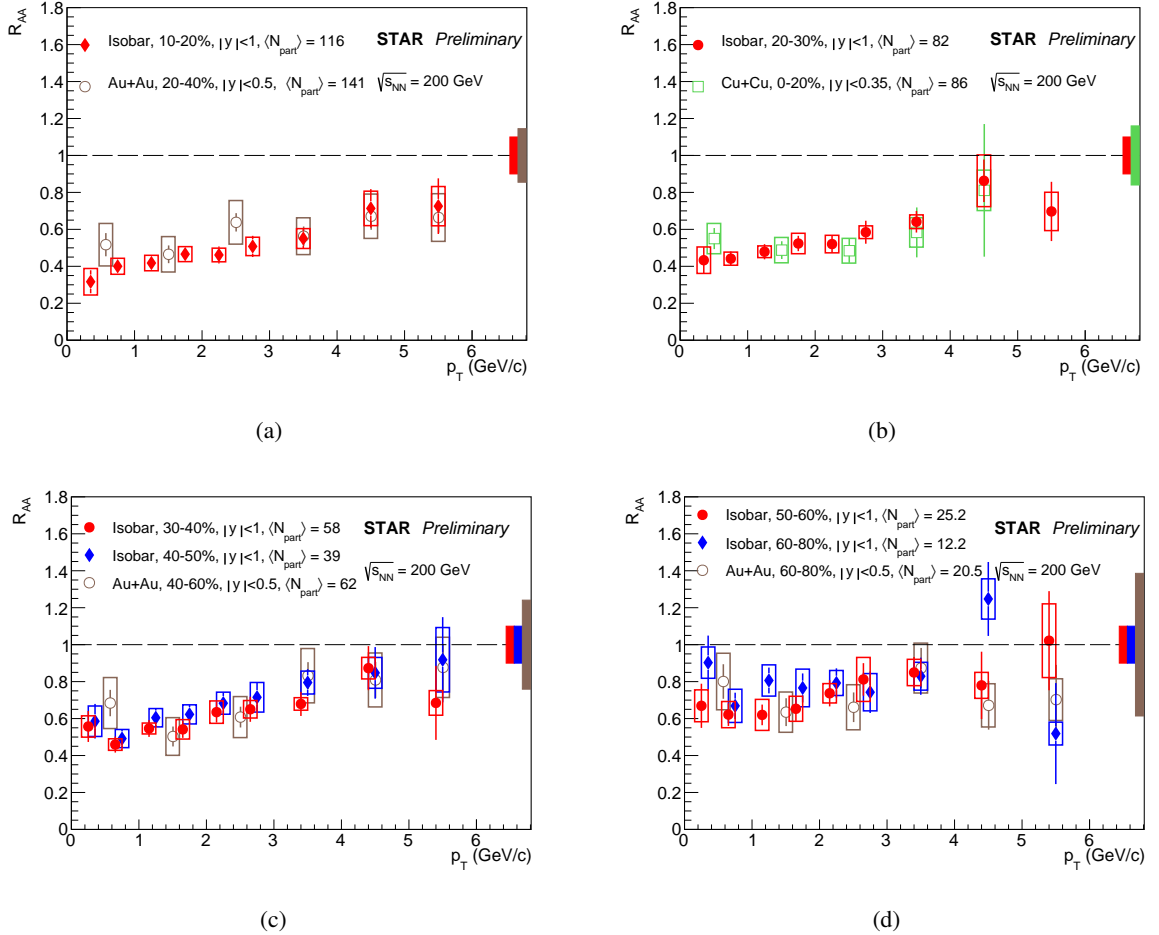


Figure 1: R_{AA} is measured as a function of p_T in 6 centralities of isobaric collisions, with the most central range in (a) and the most peripheral in (d). The statistical uncertainties are represented by the error bars, while the systematic uncertainties are denoted by the boxes. The bands around unity indicate the uncertainties originating from the T_{AA} and the $p+p$ baselines. The results are compared to similar measurements in Au+Au and Cu+Cu collisions at $\sqrt{s_{NN}} = 200$ GeV.

Figure 1 displays the nuclear modification factor R_{AA} as a function of p_T in different centralities compared with Au+Au and Cu+Cu [10, 11] results at $\sqrt{s_{NN}} = 200$ GeV with a comparable $\langle N_{part} \rangle$ range. To establish the $p+p$ baseline, measurements from both the STAR and PHENIX experiments are combined [12, 13]. The systematic uncertainties are represented by the boxes, dominated by

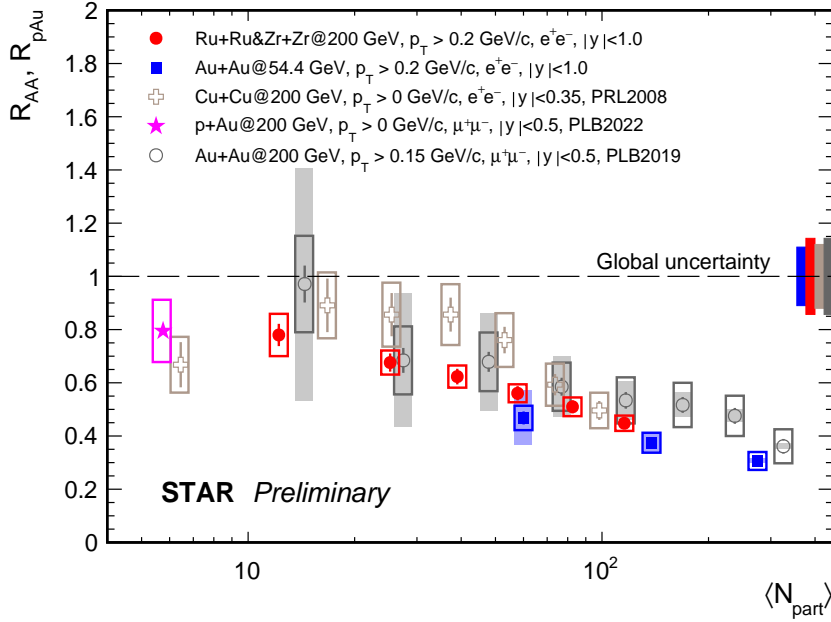


Figure 2: J/ψ R_{AA} is measured as a function of $\langle N_{part} \rangle$. The error bars represent the statistical uncertainties, while the boxes represent the systematic uncertainties. The shaded bands on the data points indicate the uncertainties from the nuclear overlap function $\langle T_{AA} \rangle$. The bands around unity indicate the uncertainties from the $p+p$ baselines.

electron matching and identification uncertainties. The main feature of these measurements is that strong suppression of the J/ψ yield is observed at central and in semi-central collisions, and no significant p_T dependence is measured in 6 centralities. In Fig. 1(a), a comparison is made between the 10 to 20% centrality in isobaric collisions and the 20 to 40% centrality in Au+Au collisions, considering the similar $\langle N_{part} \rangle$ values. The R_{AA} values in isobaric collisions are consistent with those in Au+Au collisions, but with noticeably higher precision. Similarly, in Fig. 1(b), the R_{AA} in the 20 to 30% centrality in isobaric collisions is compared with the 0 to 20% centrality in Cu+Cu collisions. The isobar results, characterized by their high precision, are also consistent with the results obtained from Cu+Cu collisions. Finally, Fig. 1(c) and Fig. 1(d) demonstrate the comparison between more peripheral isobar collisions and Au+Au collisions. Overall, the R_{AA} in isobaric collisions is consistent with those in Au+Au and Cu+Cu collisions at comparable $\langle N_{part} \rangle$ ranges.

The R_{AA} as a function of $\langle N_{part} \rangle$ is shown in Fig. 2. The red filled circles represent the isobaric collisions at $\sqrt{s_{NN}} = 200$ GeV, the blue squares correspond to Au+Au collisions at $\sqrt{s_{NN}} = 54.4$ GeV, the crosses denote Cu+Cu collisions at $\sqrt{s_{NN}} = 200$ GeV, and the star represents p +Au collisions at $\sqrt{s_{NN}} = 200$ GeV. Significant suppression is observed in the larger $\langle N_{part} \rangle$ range. All of these results consistently demonstrate a similar trend, with the degree of suppression remaining approximately constant for a given $\langle N_{part} \rangle$. This observation indicates that no significant dependence on collision system and energy is observed at RHIC energies at similar $\langle N_{part} \rangle$.

Figure 3(a) shows v_2 as a function of p_T at 0 to 80% centrality. The red markers represent

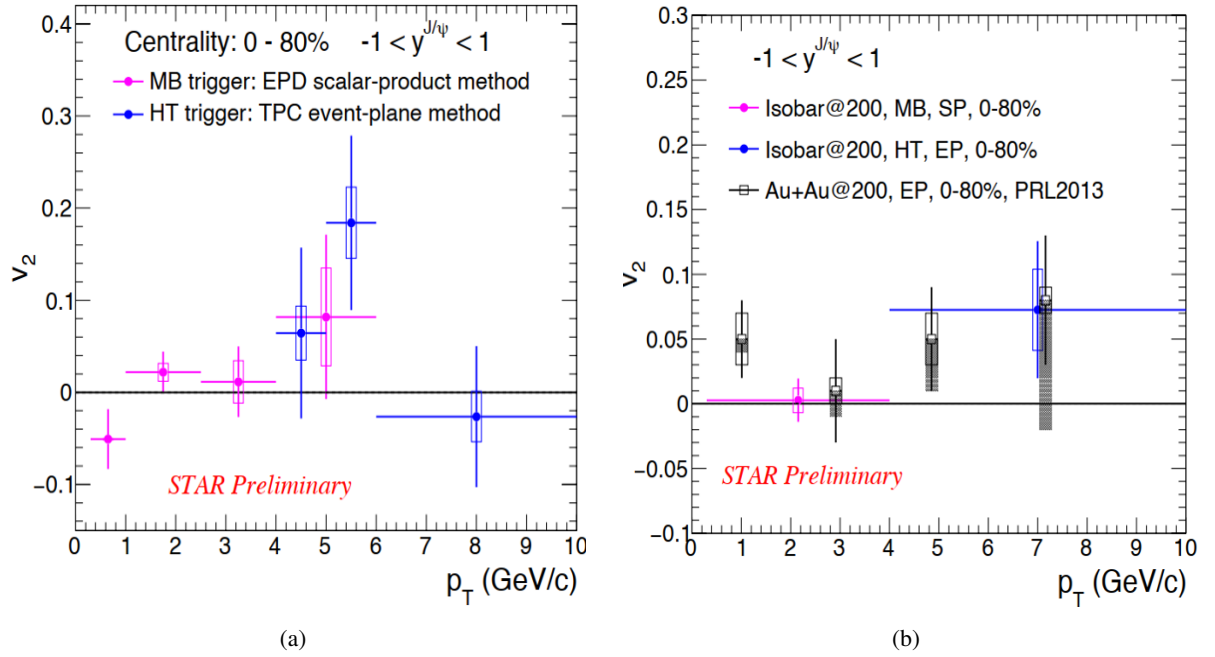


Figure 3: J/ψ v_2 as a function of p_T in the 0-80% centrality at isobaric collisions. The error bars represent the statistical uncertainties, while the boxes represent the systematic uncertainties. The results are compared to Au+Au collisions at $\sqrt{s_{NN}} = 200$ GeV, where the shaded bands on the open squares indicate the maximum non-flow.

v_2 obtained from Minimum Bias (MB) triggers using the Scalar-Product method, while the blue markers correspond to BEMC high-tower trigger (HT) results utilizing the event-plane method. These results are consistent with each other within the overlap range. The error bars represent the statistical uncertainties, while the boxes indicate the systematic uncertainties, which are dominated by electron identification and signal extraction uncertainties. No significant v_2 for the J/ψ is observed at the current level of precision. Furthermore, the result of integrating p_T over the ranges 0 to 4 GeV and 4 to 10 GeV is shown in Fig. 3(b). In the low p_T region, the most precise measurement of v_2 at RHIC to date is obtained and indicated zero J/ψ v_2 . This hints at a limited regeneration effect or small charm quark flow in isobaric collisions.

3. Conclusions

In this contribution, high-precision J/ψ R_{AA} and v_2 measurements are presented in isobaric collisions. We observe significant suppression of J/ψ in isobaric collisions at $\sqrt{s_{NN}} = 200$ GeV. No significant energy and colliding system size dependence of J/ψ R_{AA} at RHIC at similar $\langle N_{part} \rangle$ is observed. The J/ψ v_2 is consistent with zero at the current precision. This hints at a limited regeneration effect or small charm quark flow in isobaric collisions, and strong dissociation effect in central isobaric collisions.

4. Acknowledgements

This work was funded by the National Natural Science Foundation of China under Grant Nos.11720101001 and 11775213, Anhui Provincial Natural Science Foundation under Grant Nos.1908085J02.

References

- [1] Francesco Prino and Ralf Rapp. Open Heavy Flavor in QCD Matter and in Nuclear Collisions. *J. Phys. G*, 43(9):093002, 2016.
- [2] R. S. Mackintosh, A. A. Ioannides, and I. J. Thompson. Finite-range coupled reaction channel calculation of pickup contribution to the proton optical-model potential. *Phys. Lett. B*, 178:1–4, 1986.
- [3] S. Digal, P. Petreczky, and H. Satz. Quarkonium feed down and sequential suppression. *Phys. Rev. D*, 64:094015, 2001.
- [4] Shreyasi Acharya et al. *J/ψ* elliptic flow in Pb-Pb collisions at $\sqrt{s_{NN}} = 5.02$ TeV. *Phys. Rev. Lett.*, 119(24):242301, 2017.
- [5] Shreyasi Acharya et al. Study of *J/ψ* azimuthal anisotropy at forward rapidity in Pb-Pb collisions at $\sqrt{s_{NN}} = 5.02$ TeV. *JHEP*, 02:012, 2019.
- [6] L. Adamczyk et al. Measurement of *J/ψ* Azimuthal Anisotropy in Au+Au Collisions at $\sqrt{s_{NN}} = 200$ GeV. *Phys. Rev. Lett.*, 111(5):052301, 2013.
- [7] L. Adamczyk et al. *J/ψ* production at high transverse momenta in *p + p* and Au+Au collisions at $\sqrt{s_{NN}} = 200$ GeV. *Phys. Lett. B*, 722:55–62, 2013.
- [8] Sergei A. Voloshin, Arthur M. Poskanzer, and Raimond Snellings. Collective phenomena in non-central nuclear collisions. *Landolt-Bornstein*, 23:293–333, 2010.
- [9] Matthew Luzum and Jean-Yves Ollitrault. Eliminating experimental bias in anisotropic-flow measurements of high-energy nuclear collisions. *Phys. Rev. C*, 87(4):044907, 2013.
- [10] Jaroslav Adam et al. Measurement of inclusive *J/ψ* suppression in Au+Au collisions at $\sqrt{s_{NN}} = 200$ GeV through the dimuon channel at STAR. *Phys. Lett. B*, 797:134917, 2019.
- [11] A. Adare et al. *J/ψ* Production in $\sqrt{s_{NN}} = 200$ GeV Cu+Cu Collisions. *Phys. Rev. Lett.*, 101:122301, 2008.
- [12] Jaroslav Adam et al. *J/ψ* production cross section and its dependence on charged-particle multiplicity in *p + p* collisions at $\sqrt{s} = 200$ GeV. *Phys. Lett. B*, 786:87–93, 2018.
- [13] A. Adare et al. Transverse momentum dependence of *J/ψ* polarization at midrapidity in *p+p* collisions at $\sqrt{s_{NN}} = 200$ GeV. *Phys. Rev. D*, 82:012001, 2010.